TISSUE ENGINEERING: Part A
Volume 27, Numbers 13 and 14, 2021

DOI: 10.1089/ten.tea.2020.0124

termis
Tissue Engineering
& Regenerative Medicine
International Society

ORIGINAL ARTICLE

Degradation-Dependent Protein Release from Enzyme Sensitive Injectable Glycol Chitosan Hydrogel

Shalini V. Gohil, PhD,[1,2] Aiswaria Padmanabhan, MS,[3] Ho-Man Kan, MPhil,[1,2] Manakamana Khanal, PhD,[1,2] and Lakshmi S. Nair, MPhil, PhD[1–4]

Glycol chitosan (GC) is a hydrophilic chitosan derivative, known for its aqueous solubility. Previously, we have demonstrated the feasibility of preparing injectable, enzymatically crosslinked hydrogels from HPP [3-(4-Hydroxyphenyl)-propionic acid (98%)]-modified GC. However, HPP-GC gels showed very slow degradation, which presents challenges as an *in vivo* protein delivery vehicle. This study reports the potential of acetylated HPP-GC hydrogels as a biodegradable hydrogel platform for sustained protein delivery. Enzymatic crosslinking was used to prepare injectable, biodegradable hydrogels from HPP-GC with various degrees of acetylation (DA). The acetylated polymers were characterized using Fourier transform infrared and nuclear magnetic resonance spectroscopy. Rheological methods were used to characterize the mechanical behavior of the hydrogels. *In vitro* degradation and protein release were performed in the presence and absence of lysozyme. *In vivo* degradation was studied using a mouse subcutaneous implantation model. Finally, two hydrogel formulations with distinct *in vitro*/*in vivo* degradation and *in vitro* protein release were evaluated in 477-SKH1-Elite mice using live animal imaging to understand *in vivo* protein release profiles. The lysozyme-mediated degradation of the gels was demonstrated *in vitro* and the degradation rate was found to be dependent on the DA of the polymers. *In vivo* degradation study further confirmed that gels formed from polymers with higher DA degraded faster. *In vitro* protein release demonstrated the feasibility to achieve lysozyme-mediated protein release from the gels and that the rate of protein release can be modulated by varying the DA. *In vivo* protein release study further confirmed the feasibility to achieve differential protein release by varying the DA. The feasibility to develop degradable enzymatically crosslinked GC hydrogels is demonstrated. Gels with a wide spectrum of degradation time ranging from less than a week and more than 6 weeks can be developed using this approach. The study also showed the feasibility to fine tune *in vivo* protein release by modulating HPP-GC acetylation. The hydrogel platform therefore holds significant promise as a protein delivery vehicle for various biomedical and regenerative engineering applications.

Keywords: hydrogel, protein release, chitosan, subcutaneous implantation, degradation

Impact Statement

The study describes the feasibility to develop a novel enzyme sensitive biodegradable and injectable hydrogel, where in the *in vivo* degradation rate and protein release profile can be modulated over a wide range. The described hydrogel platform has the potential to develop into a clinically relevant injectable and tunable protein delivery vehicle for a wide range of biomedical applications.

[1]Department of Orthopaedic Surgery and [2]The Connecticut Convergence Institute for Translation in Regenerative Engineering, University of Connecticut Health Center, Farmington, Connecticut, USA.
[3]Department of Materials Science and Engineering, University of Connecticut, Storrs, Connecticut, USA.
[4]Biomedical Engineering Department, Institute of Material Science, University of Connecticut, Storrs, Connecticut, USA.

Introduction

Hydrogels are highly hydrated, three-dimensional networks composed of crosslinked hydrophilic polymers. Due to their high water content and physical properties which are similar to biological tissue, hydrogels have raised substantial interest for a range of pharmaceutical, biomedical, and tissue engineering applications.[1–5] The porous structure, aqueous microenvironment, biocompatibility, and biofunctionality make hydrogels interesting candidates to develop drug delivery systems, particularly for protein delivery. Studies have shown the ability of hydrogels to protect bioactive therapeutics from premature degradation.[6] As protein therapeutics are gaining momentum with more than 130 FDA (US Food and Drug Administration)-approved products and many more under development,[7] there is a significant interest in developing appropriate hydrogel carriers for the spatiotemporal release of these biologics.

Hydrogel-based carriers can be broadly classified into preformed gels and injectable gels. Preformed gels are administered via surgical intervention, whereas the injectable gels can be administered via a minimally invasive manner. Injectable hydrogels exist as polymer solutions before injection and upon injection become viscoelastic gels at the site of injection under mild physiological conditions, making them unique carriers for localized protein delivery.[8] Injectable hydrogels can be formed by physical crosslinking mediated by noncovalent interactions such as electrostatic interactions, hydrophobic interactions, and van der Waals forces as well as via host-guest interactions. These interactions are mostly regulated by external stimuli such as temperature, pH, light, electric/magnetic field, or bioactive molecules. On the contrary, several *in situ* chemical reactions such as Click reactions, Michael addition, Schiff base reactions, or enzyme or photo-mediated reactions can be used to develop covalently crosslinked injectable gels.[8]

Among these, enzyme catalyzed chemical crosslinking has many advantages as it can be performed under mild physiological conditions without unwanted side reactions, high specificity, and can occur at adjustable and fast gelation rates.[9] Several enzymes have been identified for hydrogel preparations such as transglutaminase, peroxidases, tyrosinase, laccase, as well as phosphatase.[8] Among these, plant peroxidase such as horse radish peroxidase (HRP) has been extensively investigated to develop hydrogels as injectable carriers due to their ability to support fast gelation.[10]

The release of protein encapsulated in a hydrogel matrix is governed by mechanisms such as diffusion, hydrogel swelling, hydrogel degradation, or a combination of these.[11] Hydrogels present a versatile platform to fine tune the diffusion-controlled protein release by varying parameters such as polymer properties, concentration, and crosslinking density. Since high water content and large mesh sizes can lead to rapid diffusion-controlled release, studies have also focused on designing novel hydrogels wherein the release can be tailored by other mechanisms such as molecular affinity, matrix degradation, and micro/nanoparticle as secondary carriers.[12–15]

Covalent immobilization of the drug/protein to the hydrogel matrix allows the design of carriers that support release at a rate dictated by matrix degradation.[16] Among these, enzyme-sensitive hydrogels have raised significant interest for drug delivery and tissue regeneration as their properties such as matrix swelling and degradation can be controlled using specific enzymes present in *in vivo* environment.[17] Several studies have focused on developing hydrogels that are responsive to enzymes such as matrix metalloproteinases (MMPs), which are involved in extracellular matrix remodeling.[18,19] MMP responsive hydrogels have shown the ability to undergo cell-mediated degradation as well as release the payload in a controllable manner.[20]

Chitosan is a linear polysaccharide derived from the partial deacetylation of chitin. Due to its biodegradability, biocompatibility, and solubility in aqueous media, chitosan has been widely studied for various biological and biomedical applications.[21–23] Some of its applications include wound dressing material, pharmaceutical excipients, or drug carrier and as scaffold to support tissue regeneration. In this work, a lysozyme sensitive hydrogel from acetylated glycol chitosan (GC) modified with phenol groups to allow for enzymatic crosslinking in the presence of HRP, and hydrogen peroxide was developed as an enzyme sensitive injectable hydrogel carrier for localized protein delivery.

Previous studies have demonstrated the feasibility to enzymatically crosslink phenol substituted glycol chitosan and the ability of the gel to covalently bind to proteins such as bone morphogenetic protein and retain its biological activity and induce bone formation at the site of injection.[24] However, the slow *in vivo* degradation of HPP-GC (0GC) hydrogel resulted in very little protein release and also the nondegraded hydrogel residues at the regeneration site prevented complete tissue regeneration. This warrants the need for developing hydrogels that are capable of degrading *in vivo* and support sustained protein release.

In this study, we investigated the effect of degree of acetylation (DA) on lysozyme-mediated degradation of phenol-modified glycol chitosan hydrogel *in vitro* and *in vivo*. The feasibility to tailor degradation controlled protein release from hydrogels with different DA was studied *in vitro* and *in vivo* using a subcutaneous implantation model followed by live animal imaging.

Materials & Methods

Materials

Glycol Chitosan (GC) [≥ 60% (titration), crystalline], 3-(4-Hydroxyphenyl)- propionic acid (98%) (HPP), N-3-dimethylaminopropyl-N-ethyl carbodiimide hydrochloride (EDC), N-hydroxysuccinimide (98%) (NHS), HRP, hydrogen peroxide, acetic anhydride, FITC-albumin, and lysozyme from chicken egg white were purchased from Sigma-Aldrich (St. Louis, MO). Morpholinoethanesulfonic acid (MES) powder, Spectra/Por™ Dialysis membrane, and molecular weight cutoff (MWCO) 10 kDa were procured from Scientific (Waltham, MA). Deuterium oxide (D, 99.96%) was obtained from Cambridge Isotope Laboratories, Inc. (Tewksbury, MA).

Acetylation of (Hydroxyphenyl) propionic acid modified glycol-chitosan (HPP-GC)

Aqueous carbodiimide coupling reaction was used to couple 3-(4-Hydroxyphenyl)-propionic acid to glycol chitosan (GC), as described previously.[24] The N-acetylation of the resulting polymer (HPP-GC) was achieved by using

acetic anhydride in a water/methanol solution. In brief, an aqueous solution of HPP-GC polymer (2 mL, 5% w/v) was mixed with 4 mL of methanol. The acetylating solution, composed of a freshly prepared mixture of 4 mL of methanol with variable volumes of acetic anhydride (Fig. 1), was added dropwise to HPP-GC solution and stirred vigorously for 24 h. Five sets of acetylated polymers were prepared as indicated in Figure 1 (0, 0.1, 0.3, 0.5, and 1GC), where the numbers represent the molar ratio of acetic anhydride to glucosamine units. At the end of the reaction, the reaction mixture was dialyzed against ultrapure deionized water for 3 days (with at least six changes of water) using Spectra/Por®7 Dialysis membrane, MWCO 10 kD. The reacetylated polymers were then frozen, lyophilized for 3 days and stored at −20°C until further use.

Polymer characterization

Acetylation was confirmed by attenuated total reflectance-Fourier transform infrared (ATR-FTIR) and quantitatively assessed using proton nuclear magnetic resonance (^{1}H-NMR) spectroscopic analysis of the freeze-dried polymers. The ATR-FTIR spectra for acetylated polymers were obtained in the 650–4000 cm^{-1} region, with over 200 scans, using Nicolet iS10 spectrometer (Thermo Scientific, Waltham, MA) equipped with a SMART iTX diamond ATR accessory.

The extent of acetylation was quantified using ^{1}H-NMR. The polymers ($n = 3$) were dissolved in deuterium oxide "100%" (D, 99.96%) at a concentration of 10 mg/mL and analyzed using 800 MHz Agilent VNMRS spectrometer equipped with a triple resonance HCN cold probe. NMR spectra were collected at 68°C with 8992.8 Hz bandwidth, 32 K complex data points, 128 transients, a flip angle of 90°, and 40 s recycle delay to ensure complete relaxation for proper integrations. All spectra were processed and analyzed using Mnova software from Mestrelab Research, Santiago de Compostela, Spain. Percentage DDA and DA values were calculated from the integrals of the different proton peaks using equations (1) and (2) described by Hirai *et al.*[25] Trimethyl silane (TMS) was used as reference peak. Baseline correction for each sample was done using the Bernstein correction method. Incorporation of HPP in the polymers is represented by two chemical shift peaks near 7 ppm. H0D represents solvent proton corresponding to deuterium oxide that was used for dissolving the polymers for the NMR analysis. H1D and H2D correspond to the deacetylated monomer; HAc corresponds to the acetyl group; and H3 to H6 correspond to the proton peaks.

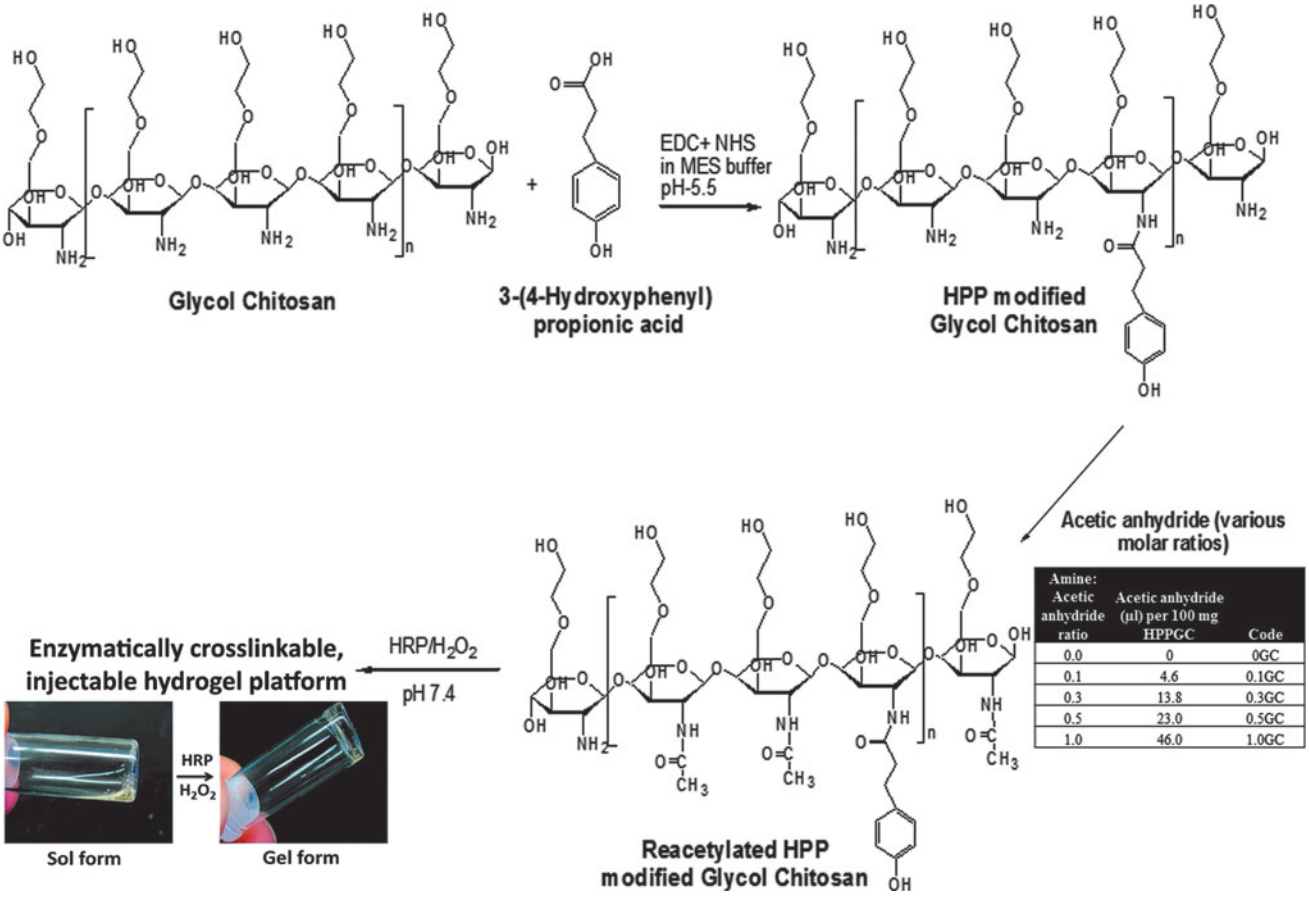

FIG. 1. Representative structures showing the chemical modification of glycol chitosan polymer via carbodiimide coupling procedure to obtain water-soluble, enzymatically crosslinkable derivative, HPP-GC. Acetylation of HPP-GC using varying amine:acetic anhydride ratios to get polymers with different degrees of acetylation. Crosslinking of acetylated HPP-GC using horseradish peroxidase and hydrogen peroxide to form injectable hydrogels. HPP-GC, 3-(4-Hydroxyphenyl)-propionic acid conjugated glycol chitosan. Color images are available online.

$$DDA\% = \left[1 - \frac{\left(\frac{1}{3}HAc\right)}{\left(\frac{1}{6}H2-6\right)}\right] \times 100 \quad [1]$$

$$DA\% = 100 - DDA\% \quad [2]$$

(where H2–6 denotes the sum of integrals of the peaks H2, H3, H4, H5, and H6)

Hydrogel preparation and characterization

The reacetylated polymers were dissolved in 1:1 w/w of water to α-MEM media, at a concentration of 20 mg/mL. HRP stock (1000 U/mL) was added to the polymer solution to obtain a final concentration of 20 U/mL. Enzymatic crosslinking was initiated via the addition of hydrogen peroxide (H_2O_2) solution to the polymer-HRP solution, at a ratio of 1:10 v/v (H_2O_2 solution: polymer-HRP solution) to obtain a final concentration of 7.349 mM. The hydrogels were analyzed for their gelation and rheological characteristics. For gelation studies, the aqueous, polymer-HRP solutions were prepared and placed in clear glass vials and gelation was initiated by quick addition and mixing of H_2O_2 solution, as described previously.[24]

Gelation or sol-gel transition was determined by tilting the vials. The sol phase was described by solution deformation and flow on tilting the glass vial, and the gel phase was described where no flow was observed. The time required for gelation was determined by visual examination of the samples before and after H_2O_2 addition. The rheological properties of the acetylated HPP-GC hydrogels (i.e., 0, 0.1, 0.3, and 0.5GC) were evaluated on Discovery HR3 hybrid Rheometer (TA Instruments, New Castle, DE), using 12 mm parallel plate geometry. All measurements were performed in the linear viscoelastic range. In brief, 110 μL of polymer solution containing HRP was conditioned (pre-shear rate: 50 rad s^{-1}; time: 10 s; gap width: 1000 mm) at 37°C, during which gelation was induced by quick addition of H_2O_2 solution, using ''gel-saver'' gel-loading pipet tips (USA Scientific, Ocala, FL). Rheological and gelation properties of hydrogels ($n = 4$) were evaluated by conducting time sweeps for 180 s at 10% strain and 1.0 Hz frequency.

Hydrogel degradation

In vitro degradation. Acetylated HPP-GC hydrogels (0, 0.1, 0.3, 0.5, and 1GC) were prepared as described in hydrogel preparation and characterization section. Upon complete gelation, each gel was transferred from the syringe mold to a preweighed glass vial and the initial weight was measured at time zero. The hydrogels were then placed in 1 mL of 50 μg/mL lysozyme in PBS (with 1% penicillin-streptomycin) and incubated at 37°C, with mild shaking. At each time point, 0.5 mL of the degradation media was removed and replaced with an equal volume of fresh media. The wet mass of hydrogel disk ($n = 4$) was determined by weighing disks after removal of excess degradation media. The gels were then lyophilized overnight, and the dry mass was determined. The *in vitro* degradation of hydrogels was evaluated in terms of ''% wet weight remaining'' and ''% dry weight remaining'' at each time point, with respect to time 0. The morphology of lyophilized hydrogels was evaluated using JEOL 6335 Field Emission Scanning Electron Microscope (SEM) operated at an accelerating voltage of 10 kV and 12 mA.

In vivo degradation using a subcutaneous implantation model. The animal study protocol was approved by the Institutional Animal Care and Use Committee (IACUC) at the University of Connecticut Health. BALB/C mice of around 21–28 g were purchased from Charles River Laboratories, Wilmington, MA and maintained in a temperature and humidity-controlled vivarium with access to rodent chow and water *ad libitum*. Before surgery, the mice were anesthetized using 1.75% isoflurane, the back was shaved using an automated shaver (Peanut WAHL®) and the skin was dabbed with 75% ethanol wipes. Four small incisions were made on the dorsal region of the mouse to make four individual pouches. In a 1 mL syringe mold, 30 μL of hydrogel was prepared and inserted into each pouch. The skin was then closed using 5-0 VICRYL® sutures. Postsurgery, a subcutaneous injection of buprenorphine was given (Supplementary Fig. S1). At predetermined time points, the animals were sacrificed by CO_2 asphyxiation. The subcutaneous skin tissue along with the hydrogel explant was collected for histology ($n = 6$). Hydrogel explant alone was also collected for gross morphological examination by SEM ($n = 2$).

For histological analysis, the samples were fixed in 10% buffered formalin for 1 day, then transferred into sucrose solution (30% w/v in PBS, pH 7.4) for 2 h. The tissue sample was placed in a plastic mold (Fisherbrand® disposable base molds) and embedded in Shandon Cryomatrix™ (Thermo Scientific). The sample was stored at −80°C until cryosectioning (7 μm cryosections) using a disposable steel blade (MX35 Premier$_+$ Thermo Scientific) on a cryostat (Leica CM 3050S). The cryosections were obtained using tape (Cryofilm type IIC^{10} section – Lab Co.) transfer method and placed on glass slides (Superfrost®Plus microscopic slides [Fisherband]). The cryosections were then transferred to clean slides smeared with adhesive (Norland optical adhesive 61) and kept at 4°C overnight followed by UV curing for 7 min. The samples were stored at 4°C until hematoxylin and eosin staining. For SEM, the hydrogel explants were washed with PBS (pH 7.4), placed at −20°C, and lyophilized. The lyophilized hydrogels were cut using thin disposable scalpel blades and placed on die-cut carbon-conductive double-sided adhesive disc (SPI supplies) attached on an aluminum stub. Before imaging, the samples were platinum-coated for improved electrical conductivity. Imaging was performed using a JEOL 6335 Field Emission SEM at 10 kV accelerating voltage and 12 μA beam current.

In vitro *and* in vivo *protein release from the hydrogels*

In vitro release studies. The release of fluorescein isothiocyanate-conjugated bovine serum albumin (FITC-BSA) from HPP-GC hydrogels with varying DAs (0, 0.1, 0.3, 0.5, and 1GC) was evaluated under three release conditions viz. PBS, 10 μg/mL lysozyme in PBS, and 50 μg/mL lysozyme in PBS. One percent penicillin-streptomycin solution was added to all release media to prevent bacterial and fungal contamination. For hydrogel preparation, the polymers were dissolved in 50:50 ratio of water:α-MEM to

obtain a final polymer concentration of 20 mg/mL. HRP stock (1000 U/mL) and FITC-albumin was added to the polymer solution to obtain a final concentration of 20 U/mL and 5 mg/mL, respectively. The FITC-Albumin-polymer-HRP solution (180 μL) was added into syringe mold, and gelation was induced by the addition of H_2O_2, as discussed in hydrogel preparation and characterization section. Blank hydrogel discs (without FITC-albumin) were also prepared as controls for each release condition. Each hydrogel disc ($n = 4$ per group) was then incubated in 3 mL release medium at 37°C with gentle rocking. At each time point, 1.5 mL of the release medium was removed and replaced with an equal volume of fresh release medium. The FITC-albumin released at each time point was quantified using UV spectroscopy analysis at 495 nm. A standard curve of FITC-albumin dissolved in each of the release media was used as a standard for quantification. Absorbance values were normalized against unloaded control samples.

In vivo release evaluation by live animal imaging studies. The animal study protocol was approved by the Institutional Animal Care and Use Committee (IACUC) at the University of Connecticut Health. 477-SKH1-Elite Mouse Crl: SKH specific hairless, pathogen-free male mice of around 25–30 g were purchased from Charles River Laboratories (Wilmington, MA) and maintained in a temperature and humidity controlled vivarium with access to rodent chow and water *ad libitum*. Sulfatrim® (Sulfamethoxazole/Trimethoprim), an antibiotic, was administered daily for 7 days before surgery. Animals were individually caged to prevent from possible skin infections.

Hydrogels (0.1 and 0.5GC) loaded with Cy-7 conjugated BSA (Cy7-BSA; Nanocs, Inc.) were prepared as described in hydrogel preparation and characterization section. The gels were then implanted into the subcutaneous pouch created at the lower dorsal region of mouse (one gel per animal, 8 animals per group). Hydrogel without Cy7-BSA was used as a control ($n = 3$ for each polymer). *In vivo* imaging studies were performed using an IVIS® Spectrum system (PerkinElmer, Waltham, MA). After the final imaging time point, the mice were euthanized and the skin and hydrogel (if any) at the implantation site was isolated, fixed, and assessed by histology, as described in *in vivo* degradation using a subcutaneous implantation model.

Results & Discussion

Synthesis and characterization of acetylated HPP-GC polymers

Properties of chitosan such as biocompatibility, mechanical strength, and biodegradability can be tuned by varying the DA of the polymer. Acetic anhydride is commonly used to increase the DA of chitosan.[26] Acetylation of chitosan by acetic anhydride involves reaction between the nucleophilic unprotonated primary amino group of glucosamine and one carboxyl function in the acetic anhydride.[26] The acetic anhydride-based method causes selective N-acetylation in chitosan and does not produce toxic by-products. Since it involves a mild reaction, this method also helps to retain and preserve the inherent biological properties of the polymer.[26]

In this study, phenol groups were first added to glycol chitosan polymer chains by carbodiimide-mediated coupling of HPP as described in our previous work.[24] Polymers with different degrees of acetylation (DA) were obtained by reacting HPP-GC with varying acetic anhydride concentrations. Figure 1 shows the HPP coupling, acetylation, and enzymatic crosslinking processes used to obtain acetylated HPP-GC hydrogels. Followed by purification and lyophilization, the polymers were obtained in the form of fluffy white solids. FTIR and ^{1}H-NMR (Fig. 2) confirmed the formation of acetylated HPP-GC polymer. The ATR-FTIR spectra of the acetylated polymers showed all the characteristic peaks of HPP-GC as reported in our previous study.[24] An additional peak was observed at 1653 cm^{-1} corresponding to C=O group from secondary amide, due to the acetylation of glycol chitosan polymer chain, similar to that reported for acetylated chitosan.[27,28] Increase in intensity of C=O peak (Fig. 2A) indicates increase in the DA of polymers treated with acetic anhydride. However, since the bands overlap with primary amine and polysaccharide bands, it does not fully correlate to the DA for quantitative analysis.[29]

^{1}H-NMR (Fig. 2B) was therefore used to quantitatively determine the DA of the acetylated HPP-GC polymers. As shown in the figure, as the amount of acetic anhydride was increased, the percentage DA of the polymers increased, demonstrating the dependence of the acetylation of the polymer on the acetic anhydride concentration. However, even for 1GC, the extent of acetylation obtained for glycol chitosan was only ~35%. Similar to chitosan, an excess amount of acetic anhydride may be required to achieve more than 50% acetylation of HPP-modified glycol chitosan as the reaction was performed in aqueous media.[30] Moreover, the presence of HPP groups in glycol chitosan may also limit the acetylation reaction when performed at room temperature.

Fabrication and characterization of acetylated HPP-GC hydrogels

The acetylated HPP-GC polymers underwent enzymatic gelation under the same conditions as that of HPP-GC. All the polymers showed gelation in less than 90 s, accompanied by syneresis (Supplementary Fig. S2). The DA did not significantly affect the HRP-mediated gelation time of HPP-GC in the presence of H_2O_2. This can be attributed to the very fast enzymatic gelation process under the tested gelation conditions. However, rheological behavior of the hydrogels (Fig. 3) showed dependence of storage modulus of the hydrogels on the DA. N-aceyl glucosamine content in chitosan has shown to influence hydrophobic interactions between polymer chains leading to polymer chain self-association and thereby increasing the storage modulus of resulting hydrogels.[31] The enzymatic hydrogels prepared using acetylated glycol chitosan showed an increase in the storage modulus with increase in the DA. The 0.3 and 0.5GC hydrogels showed significantly higher storage modulus compared to 0 and 0.1GC. These data show increased polymer chain interactions with increase in N-acetyl glucosamine content in HPP-GC hydrogels.

In vitro *and* in vivo *degradation of the acetylated HPP-GC hydrogels based on lysozyme concentration*

Biodegradable materials undergo *in vivo* degradation mainly via enzymatic or hydrolytic processes. Chitosan is known to undergo enzymatic degradation in presence of

enzymes such as lysozyme and chitinase.[32] Lysozyme is present in human body, particularly in tears, serum, and saliva. Acute/chronic inflammation resulting from injury or surgical procedure can also result in the secretion of lysozyme by neutrophils and macrophages. Unlike lysozyme, the presence of chitinase in humans is associated with disorders such as infection, asthma, and allergy.[33,34] Therefore, lysozyme plays the central role in enzyme-mediated degradation of acetylated chitosan in humans. Degradation of chitosan occurs by lysosome-mediated lysis of the polymer chains at the acetyl functionality. Similar to chitosan, the degradation rate of the HPP-GC polymers in the presence of lysozyme is expected to increase concurrently with the DA of the polymer. To test this hypothesis, *in vitro* degradation of acetylated HPP-GC hydrogels was evaluated in the presence of 50 μg/mL lysozyme. The rate of lysozyme-mediated degradation of the HPP-GC polymers was found to be dependent on the DA. As shown in Figures 4A and B, the 0.5GC hydrogel (DA 31.7%) showed complete degradation in less than 65 h, whereas the 0.3GC hydrogel (DA 28.03%) showed complete degradation in less than 120 h. On the contrary, 0GC (~7%) and 0.1GC (~16%) hydrogels showed less than 20% dry weight decrease in 200 h. This shows the significant impact of more than 20% DA of HPP-GC on hydrogel degradation. Despite their low DA, the data, however, show the potential long-term degradability of 0 and 0.1GC hydrogels. Interestingly, the wet weight of 0GC hydrogels showed significant decrease compared to 0.1GC during the 200 h degradation study.

N-acetylation of chitosan has shown to increase the amorphous regions within the gel structure, thereby increasing water permeation, swelling, and degradation.[35] The increase in wet weight of 0.1GC hydrogel compared to 0GC is presumably due to the increase in swelling of the hydrogel along with slow degradation. The increased wet weight of 0.3GC hydrogel till 65 h is also presumably due to increased swelling along with significant degradation. Another confounding factor in the study is that these gels showed synerisis during gelation with 0GC showing the highest water loss compared to the acetylated gels. Lower dry weight of 0GC compared to 0.1GC is presumably due to the difference in synerisis and hence accompanying polymer loss during gelation. Figure 4C shows the cross-sectional morphology of the hydrogels as a function of time in the presence of lysozyme. The hydrogels, irrespective of the DA, showed a highly porous morphology. Similar to other chitosan hydrogels,[35] the acetylated glycol chitosan hydrogels also showed a decrease in the number of pores and formation of a sheet-like internal structure upon enzymatic degradation. Morphological observation also implies a surface erosion mechanism wherein the size and mass of the gels decreased with time.

To evaluate the *in vivo* degradation profiles, the hydrogels were implanted subcutaneously and their gross morphology was studied using SEM imaging of the explanted samples at predetermined times. Figure 5A shows SEM images of the explanted hydrogels along with the surrounding fibrous tissue at various time points postimplantation. At week 1, the hydrogels (0, 0.1, 0.3, and 0.5GC) were intact at the implanted site surrounded by a fibrous sheath. The 1.0GC hydrogel, however, showed significant disintegration at that time point. The cross-sectional morphology of the explanted and lyophilized hydrogels presented a porous structure. Even at 6 weeks postimplantation, both 0 and 0.1GC hydrogels were largely intact at the site of implantation. Similar to the trend observed in the *in vitro* degradation study, the 0.3 and 0.5GC hydrogels showed significant *in vivo* degradation compared to 0 and 0.1GC hydrogels. Smaller residues of the 0.3 and 0.5GC hydrogels were present at the site of implantation at 2 weeks postimplantation. On the contrary, at 2-week time point, no gel residue can be found for 1.0GC hydrogel. The data support the *in vitro* data, wherein the degradation rate of the acetylated HPP-GC gel was found to be related to the polymer's DA.

This was further supported by the histological analysis of the explanted tissue. Figure 5B shows the H&E-stained sections of acetylated HPP-GC hydrogels and the surrounding tissue as a function of time postimplantation. Positively charged intact chitosan stains reddish pink by eosin in physiological conditions. Negatively charged degraded chitosan stains blue by hematoxylin.[36] Sham group at week 1 showed significant cellular infiltration, due to the acute inflammatory phase that followed the surgical incision. However, the inflammatory cell infiltrate disappeared by week 2 and normal skin tissue morphology was observed. Condition of the sham sample at weeks 4 and 6 was similar to that at week 2, demonstrating that the acute inflammatory phase had subsided by week 1 and complete healing was observed by week 2. At week 1, the 0GC hydrogel was intact under the skin surrounded by a thin fibrous capsule containing inflammatory cells. Tissue response at week 2, 4, and 6 were similar to that at week 1, with largely intact hydrogel present under the skin. Cell infiltration was minimal, and presence of fibrous sheath with cell activity was observed. At week 1, the 0.1GC hydrogel was intact with a thin fibrous layer and minimal cell infiltration. At weeks 2 and 4, the hydrogel was largely intact, but the presence of cellular activity in the fibrous sheath was found to be more profound compared to the 0GC hydrogel. Furthermore, the 0.1GC hydrogel showed more signs of disintegration at week 6 compared to the 0GC hydrogel at the same time point. The data show the potential for faster *in vivo* degradation of 0.1GC hydrogel compared to 0GC. The 0.3 and 0.5GC hydrogels showed cellular infiltration and significant matrix degradation as evidenced by blue stained chitosan residues at weeks 1 and 2. By week 4, complete degradation of the hydrogels was observed for both 0.3 and 0.5GC hydrogels along with absence of inflammatory

FIG. 2. **(A)** Overlay of representative ATR-FTIR spectra of glycol chitosan and reacetylated HPP-GC polymers (0, 0.1, 0.3, 0.5, and 1GC). **(B)** Overlay of representative proton-NMR spectra of recaetylated polymers (0, 0.1, 0.3, 0.5, and 1GC) showing the % DA calculated using integral values of individual peaks corresponding to protons of acetylated (A) and deacetylated (D) monomer. The high magnification shows the changes in chemical shifts of H2D (~2.85 ppm) and CH_3 HAc (2.05 ppm) protons, with increasing DA of the reacetylated polymers. TMS was used as the reference. HOD refers to the peak for deuterium oxide. TMS, trimethyl silane; ATR-FTIR, attenuated total reflectance-Fourier transform infrared. Color images are available online.

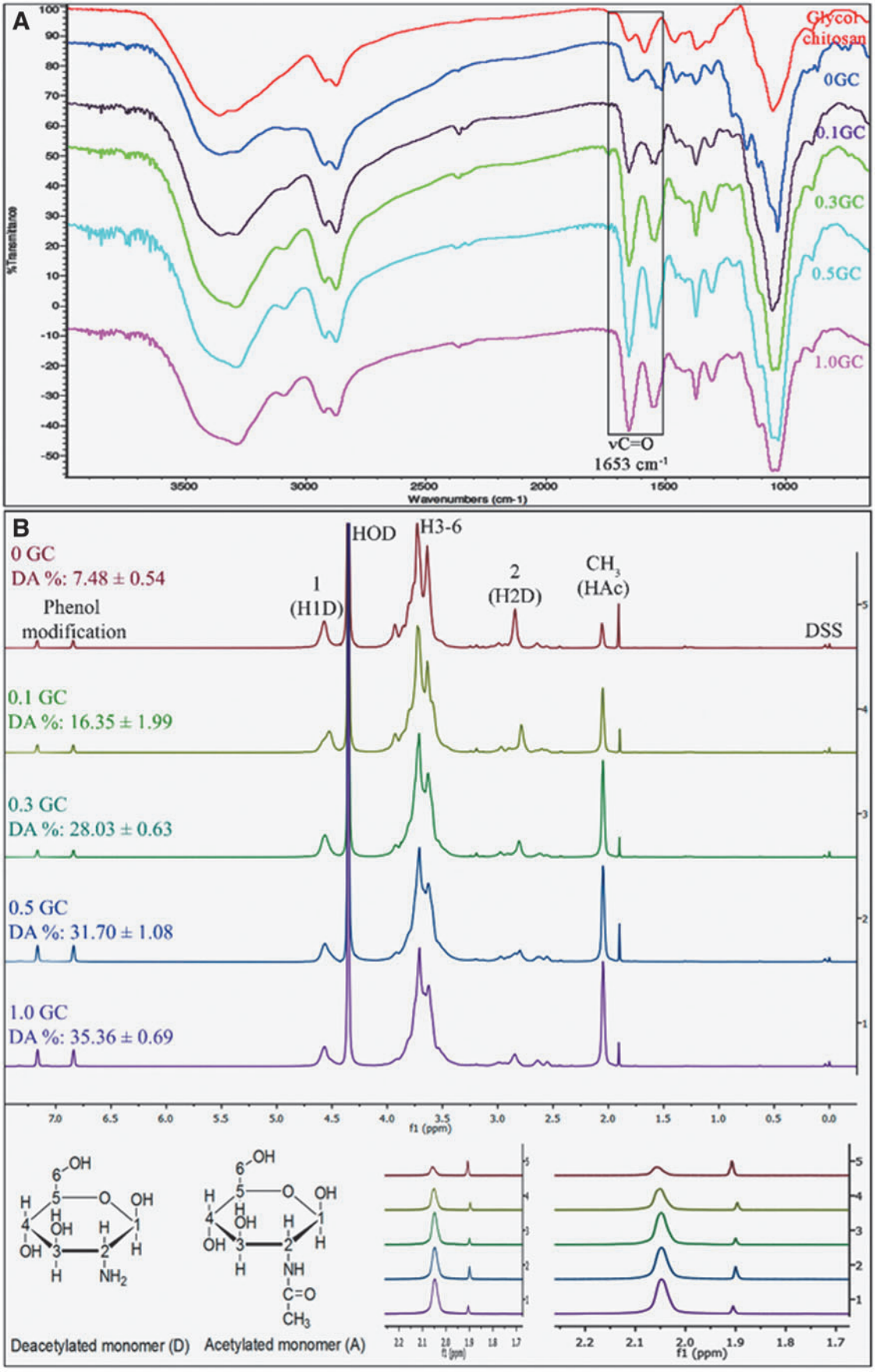
A
Glycol chitosan
0GC
0.1GC
0.3GC
0.5GC
1.0GC
%Transmittance
vC=O
1653 cm-1
Wavenumbers (cm-1)
B
0 GC
DA %: 7.48 ± 0.54
Phenol modification
1 (H1D)
HOD
H3-6
2 (H2D)
CH3 (HAc)
DSS
0.1 GC
DA %: 16.35 ± 1.99
0.3 GC
DA %: 28.03 ± 0.63
0.5 GC
DA %: 31.70 ± 1.08
1.0 GC
DA %: 35.36 ± 0.69
f1 (ppm)
Deacetylated monomer (D)
Acetylated monomer (A)

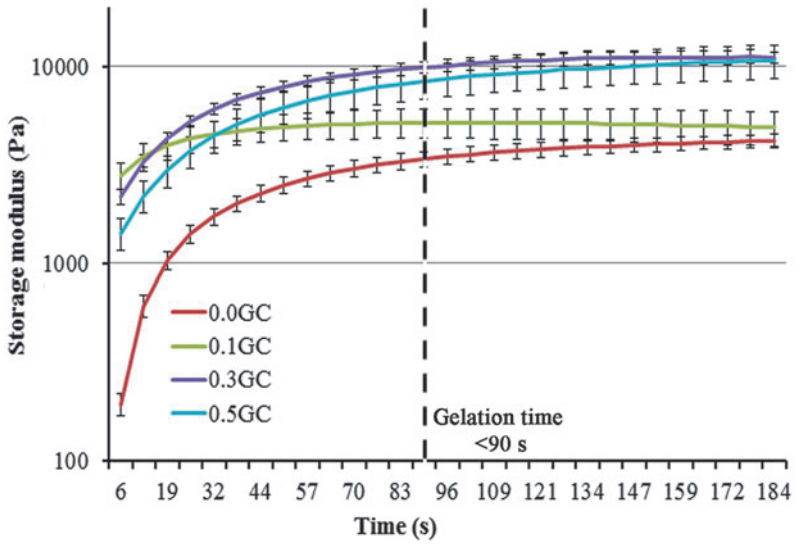

Sample code	Storage modulus (Pa)
0GC	4022.5 ± 328.8
0.1GC	5065.4 ± 963.5
0.3GC	10999.9 ± 847.7
0.5GC	10185.6 ± 2029.9

FIG. 3. Dynamic rheological evaluation showing, time-dependence of storage modulus of reacetylated HPP-GC hydrogels (0, 0.1, 0.3, and 0.5GC). The table shows the average storage modulus of the hydrogels. Color images are available online.

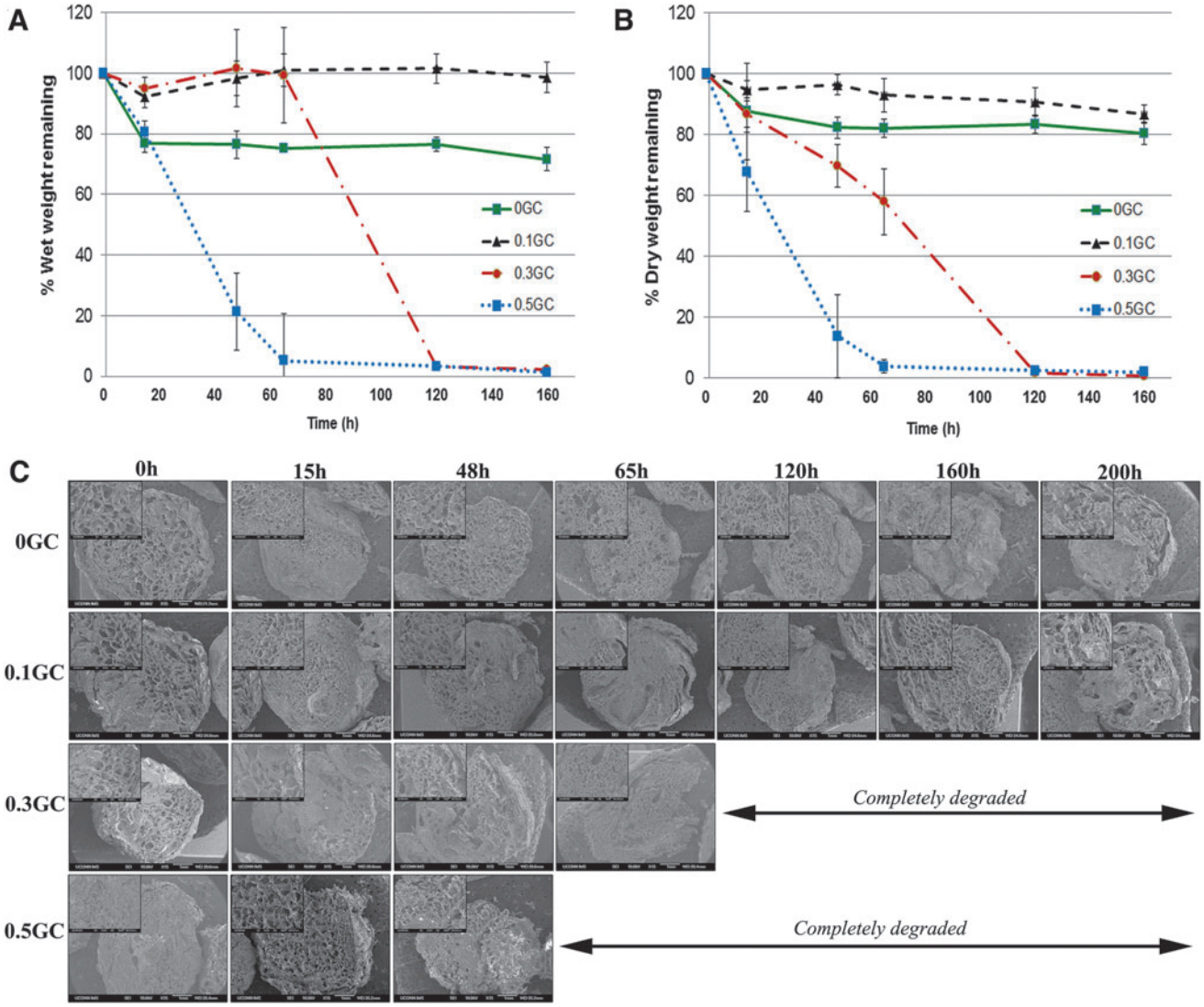

FIG. 4. *In vitro* degradation studies showing **(A)** % wet weight remaining; **(B)** % dry weight remaining; and **(C)** morphological changes in the hydrogel discs with time; for the reacetylated glycol chitosan hydrogels (0, 0.1, 0.3, and 0.5GC). Color images are available online.

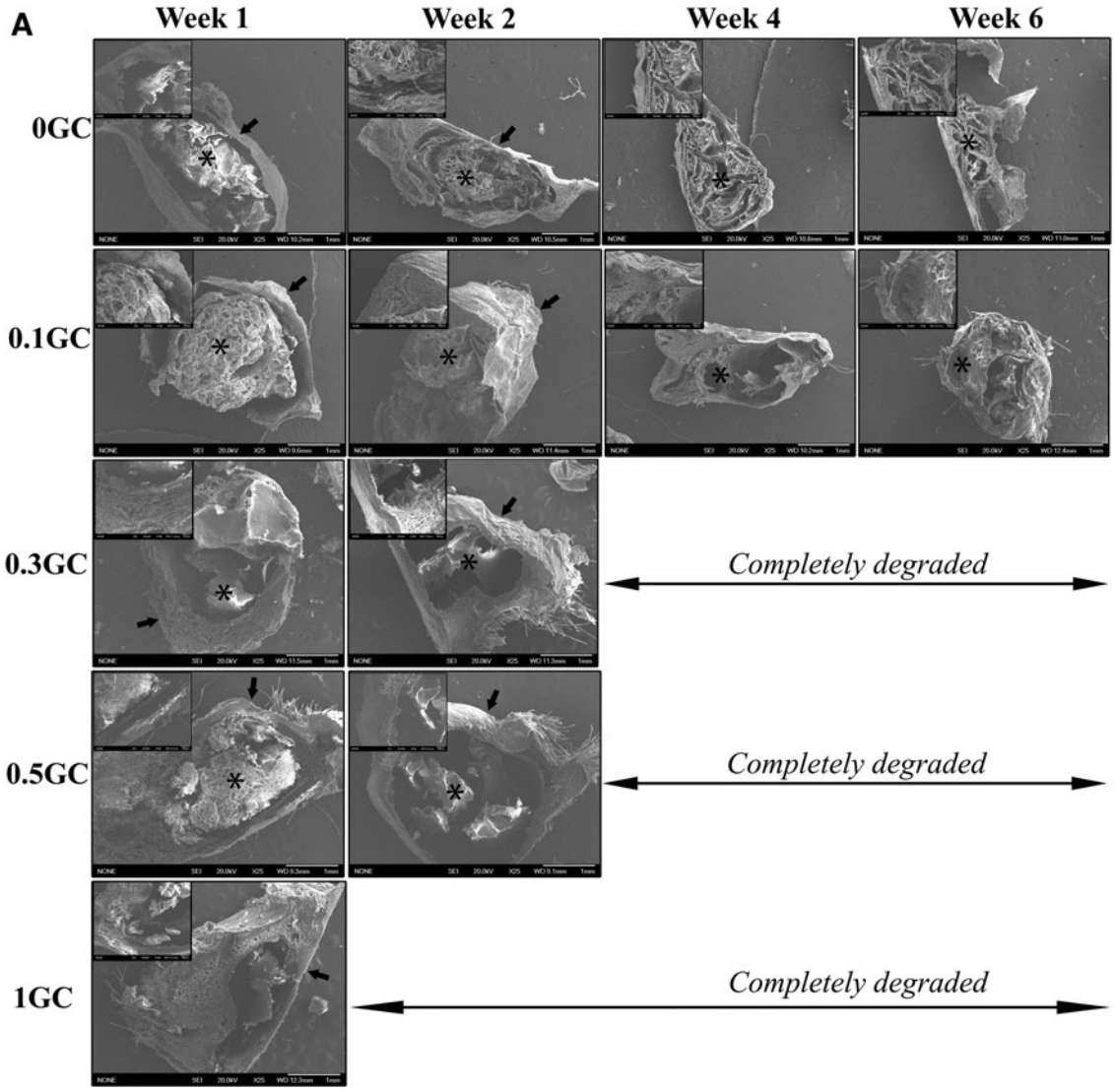

FIG. 5. **(A)** Representative gross morphology of explanted hydrogels by SEM (25×, inset 100×). *Sign indicates the GC hydrogel, *Arrow* indicates the fibrous layer surrounding the hydrogel. **(B)** Representative image of hematoxylin and eosin-stained sections of explanted hydrogels at different time points. Color images are available online.

cellular response. In the case of 1GC gels, even at week 1, only small residues of the hydrogel can be identified along with degraded chitosan matrix (stained blue) and by week 2, complete degradation of the gel observed with lack of any inflammatory cell response.

The mechanism of chitosan hydrogel degradation involves the secretion of lysozyme by inflammatory cells such as neutrophils and macrophages that infiltrate the hydrogels. The degraded hydrogels are then ingested by the macrophages. As discussed before, the N-acetyl groups play a significant role in the *in vivo* degradation of chitosan, and an increase in N-acetyl groups leads to faster polymer degradation *in vivo*. The *in vivo* degradation rate of the acetylated HPP-GC hydrogels increased with increase in DA, confirming the role of N-acetyl groups in HPP-modified glycol chitosan degradation. Even though the gels underwent a cell-mediated degradation, a thin fibrotic capsule was observed around the gels during the early stages of degradation with minimal inflammatory response and upon gel degradation, the implantation site appeared similar to that of sham implying the tissue compatibility of the hydrogels. A previous study using chitosan crosslinked with glutaraldehyde for brachytherapy showed that, at 14 and 28 days post-implantation, the chitosan gels showed thin fibrous capsule formation with minimal inflammatory response compared to the pronounced inflammatory response observed for the biodegradable suture ''Vicryl,'' indicating the general biocompatibility of chitosan-based gels.[36] The *in vivo* tissue response toward a chitosan derivative [chitosan-poly(butylene succinate)]-based fiber mesh was previously evaluated.[37] The study concluded that the implants elicited normal immune response upon implantation along with degradation by 12 weeks, further supporting the general tissue compatibility of chitosan-based matrices. Another study by Tomihata and Ikada using deacetylated chitin films via subcutaneous implantation demonstrated that the *in vivo* degradation rate was dependent on the extent of acetylation and that the deacetylated chitin showed mild tissue response.[38]

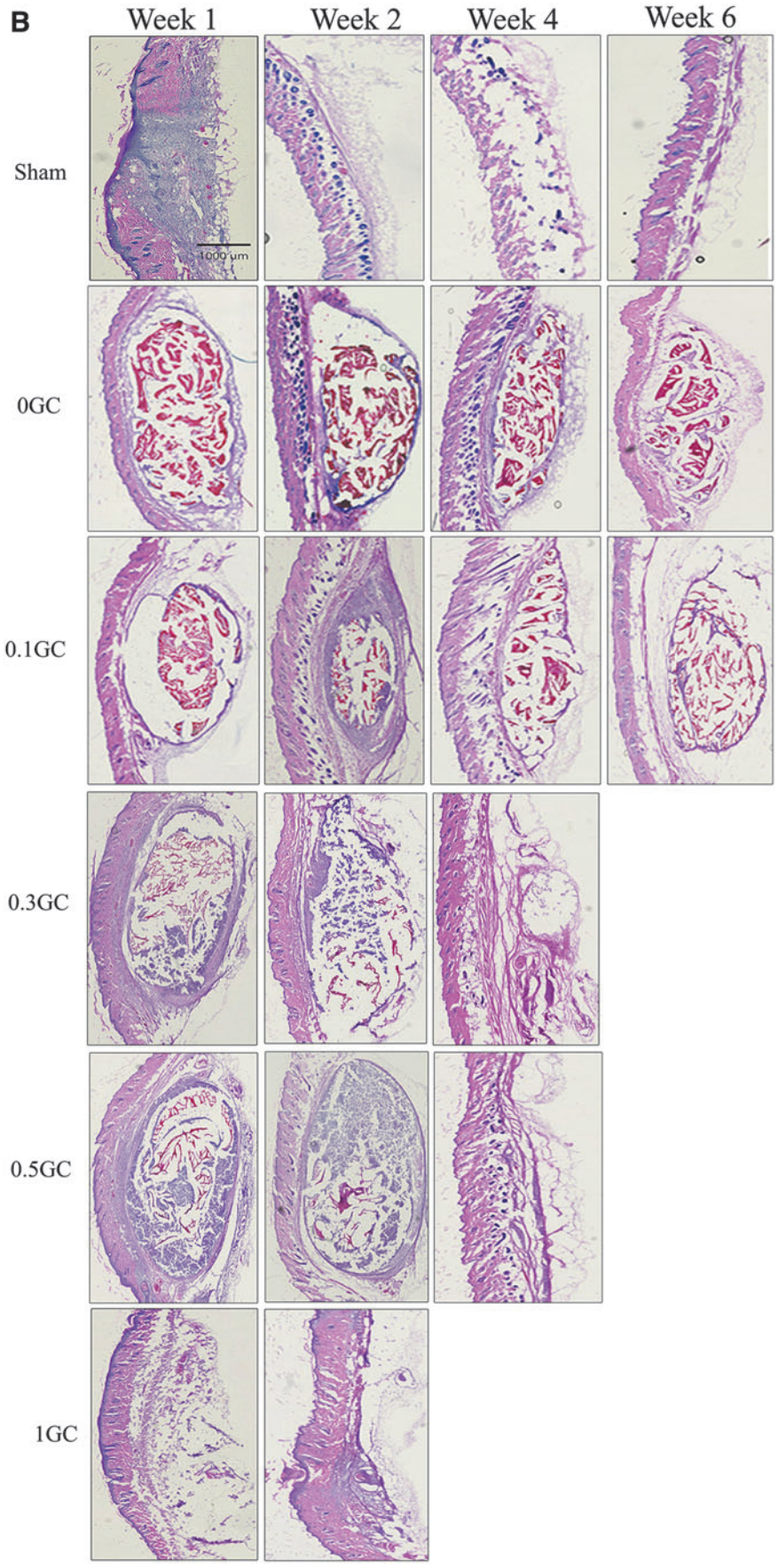

FIG. 5. (*Continued*)

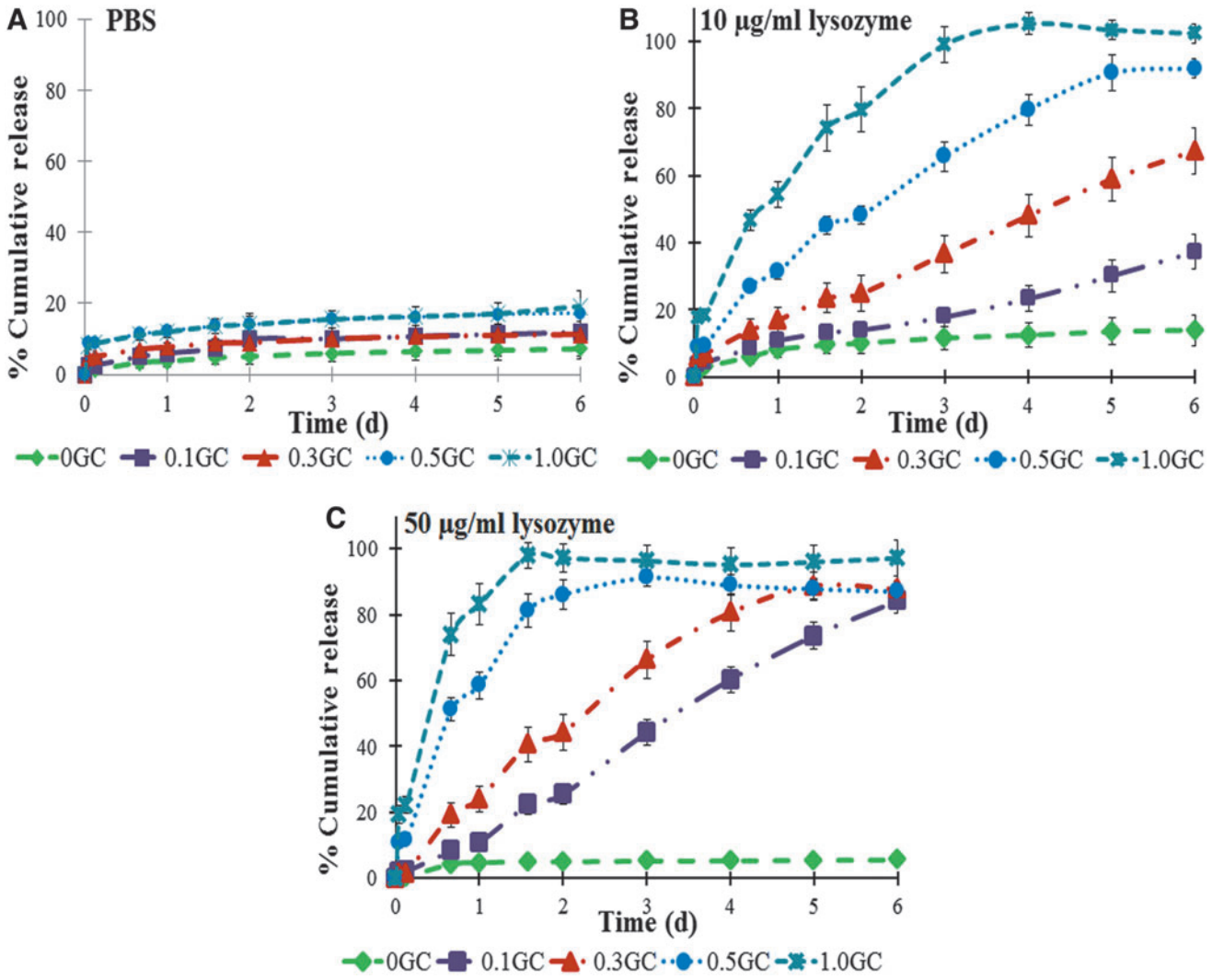

FIG. 6. *In vitro* release showing the release of FITC-albumin in various release conditions. **(A)** PBS alone, **(B)** 10 µg/mL lysozyme in PBS, and **(C)** 50 µg/mL lysozyme in PBS. Color images are available online.

In vitro *and* in vivo *protein release from acetylated HPP-GC hydrogels*

Our previous study[24] showed very little release of encapsulated growth factors from HPP-GC (0GC) hydrogels in PBS. This study therefore evaluated the effect of DA of HPP-GC hydrogels on protein release in the presence of lysozyme. FITC-conjugated bovine serum albumin (FITC-BSA) was used as a model protein to understand the efficacy of controlling the degradation-mediated protein release from acetylated HPP-GC gels. *In vitro* protein release was first carried out in PBS to determine the effect of hydrogel DA on diffusion-controlled protein release. Figure 6A shows the cumulative BSA release profile from acetylated HPP-GC hydrogels in PBS. As it can be seen, all the gels, irrespective of their DA showed a burst release, followed by a lack of significant protein release over time. The data indicate significant interaction of the protein to the HPP-GC hydrogel independent of DA.

Our previous study[39] using alginic acid and hyaluronic acid showed significant retention of BSA in phenol-mediated enzymatically crosslinked hydrogels. Albumin is a globular protein with several tyrosine residues and the FITC molecule contains a phenol functional group. The phenol groups in FITC-albumin could participate in the enzymatic crosslinking process causing the protein to be chemically conjugated to the gel matrix, resulting in the very low release of the protein as observed in the present study. Moreover, no statistically significant differences were observed in the diffusion-controlled protein release from gels of different DA, implying that irrespective of the DA, protein conjugation can happen.

Subsequent study therefore investigated whether a degradation-dependent release kinetics can be achieved from this hydrogel platform. The study was performed by incubating the FITC-albumin-loaded acetylated HPP-GC hydrogels in PBS containing 10 and 50 µg/mL of lysozyme at 37°C. Figures 6B and C show the cumulative release of FITC-albumin from the hydrogels in presence of lysozyme as a function of time. In the 10 µg/mL lysozyme group, the 0GC hydrogel did not show significant release of FITC-albumin, with the release profile being similar to that in PBS. However,

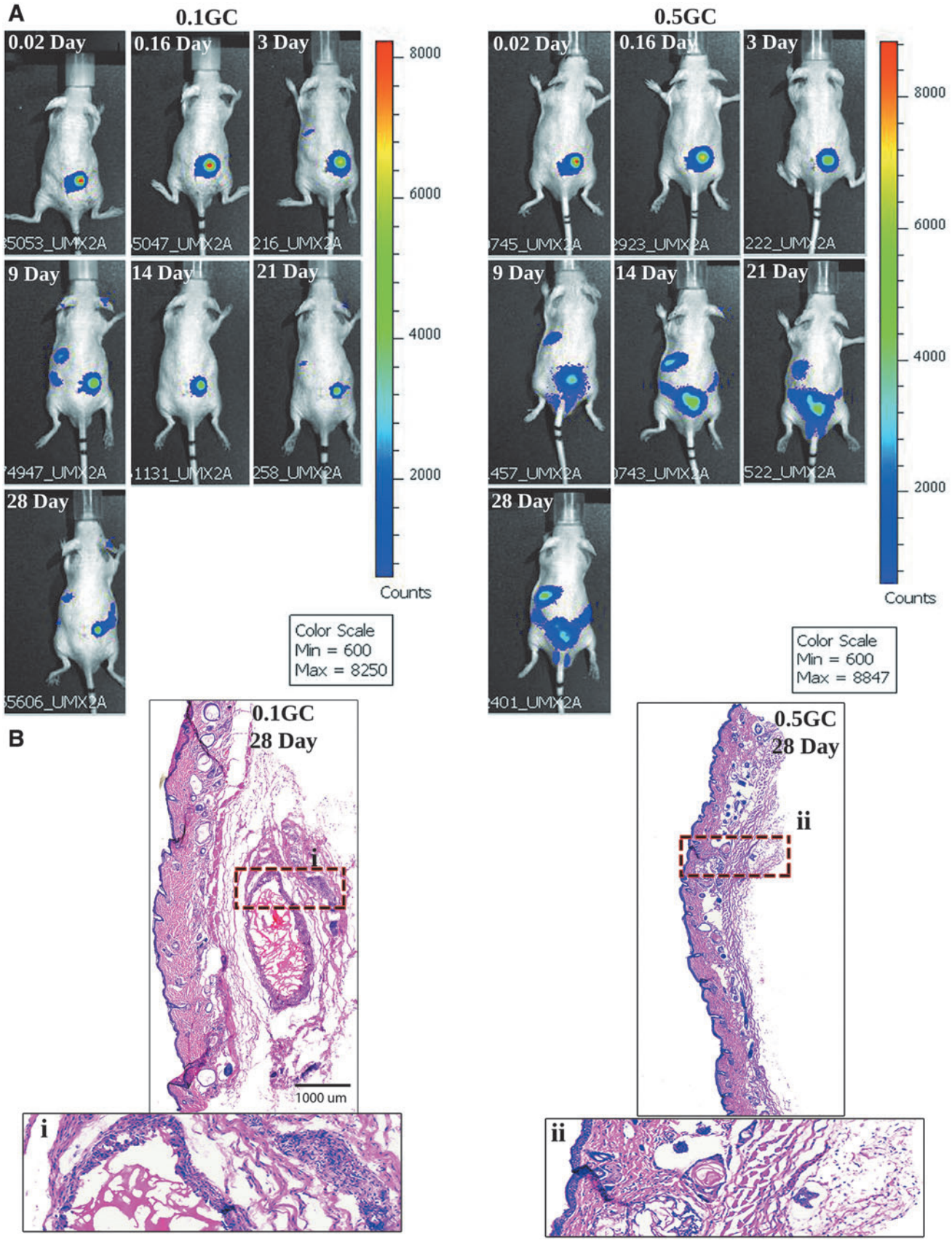

FIG. 7. *In vivo* release profile of Cy7-BSA-loaded acetylated HPP-GC hydrogel as a function of time. **(A)** Live animal imaging and **(B)** representative images of hematoxylin and eosin-stained sections of explanted hydrogels at 28 days postimplantation. Color images are available online.

the percentage release increased with increasing DA (0.1–1.0GC), with the 1GC hydrogel showing complete release ($\sim$100%) at day 3. By day 6, unlike in PBS, in the presence of lysozyme, the various gels tested (0.1, 0.3, 0.5, and 1GC) showed significant protein release. Moreover, the gels showed distinct release profiles demonstrating the effect of DA on degradation-mediated protein release. The data show the feasibility of achieving a wide range of degradation-mediated protein release profiles by varying the DA of HPP-GC hydrogels.

To understand the effect of lysozyme concentration on protein release from acetylated HPP-GC hydrogel, another release study was performed using 50 μg/mL lysozyme (Fig. 6C). Even in 50 μg/mL, the 0GC hydrogel showed no significant difference in release profile compared to that observed in PBS or in the presence of 10 μg/mL lysozyme. However, the percentage release values for the other hydrogels (0.1–1.0GC) increased in comparison to those in 10 μg/mL lysozyme environment, with the 1.0GC hydrogel showing a percentage release value of about $\sim$97.97% in 38 h. The data show the feasibility to further modulate drug release by varying the lysozyme concentrations. Since most of the protein-based drugs have tyrosine residues, it is possible to achieve a degradation-mediated release of many of the biologics using these enzymatically crosslinked hydrogels. Our previous studies demonstrated the potential of HPP-GC (0GC) to bind and retain the biological activity of growth factors such as bone morphogenetic proteins to induce bone formation *in vivo*.[24] The acetylated HPP-GCs present the feasibility not only to encapsulate proteins in a biologically active manner but also to release protein at different rates depending on the DA.

In vivo release study using live animal imaging studies. Live animal imaging was utilized to understand the degradation-dependent *in vivo* release of protein from acetylated HPP-GC hydrogels. Based on the *in vitro* protein release study discussed above, 0.1 and 0.5GC hydrogels were selected as representative of slow and fast degrading gels, respectively. The hydrogels were loaded with Cy7-BSA for live animal imaging. Figure 7A shows the images comparing 0.1 and 0.5GC, at different time points. As can be seen, the fluorescent signal remained localized at the implantation site for both the gels during the early time points. However, by day 9, 0.5GC gels showed significant bleeding of the Cy7-BSA compared to 0.1GC gels. The degradation-mediated release from 0.5GC is further indicated by the presence of signal intensity in the liver as BSA is metabolized in liver. In the case of 0.1GC gels, even at day 28, the signal intensity is mostly observed at the site of implantation, showing very low hydrogel degradation as also evidenced from histological analysis (Fig. 7B). Despite the faster degradation of 0.5GC, even at day 28, some signal intensity was observed at the site of implantation. The histological analysis (Fig. 7B) showed the presence of small residues of the hydrogels unlike the previous data (Fig. 5B). This is presumably due to the additional crosslinking due to the presence of BSA. The results show that the *in vivo* localization of the protein can be tuned effectively by varying the DA of HPP-GC hydrogels. The present study demonstrated that HPP-GC hydrogels can show a wide range of degradation behavior dependent on the DA of the starting polymer and could be used in the development of tailored hydrogels for a variety of regenerative applications.

Conclusions

We demonstrated the feasibility to develop injectable enzymatically crosslinked hydrogels from acetylated HPP-GC that degrade over wide period of time depending on the DA. The HPP-GC polymers showed fast gelation times (<90 s) independent of the extent of acetylation. Both *in vitro* and *in vivo* degradation studies showed that increase in the DA can led to concomitant increase in degradation rate with 1.0GC exhibiting complete degradation in 1 week. *In vitro* release study in PBS alone demonstrated minimal diffusion-controlled release and the ability of the hydrogels to retain the encapsulated protein within the gel independent of the DA. In the presence of lysozyme, degradation-controlled release of protein was observed, and the rate of protein release was dependent on the DA. The study demonstrated that the degradation and subsequent protein release from enzymatically crosslinkable acetylated glycol chitosan hydrogels can be controlled by varying the DA as well as lysozyme concentration and therefore hold tremendous potential for developing engineered protein delivery vehicles.

Disclosure Statement

No competing financial interests exist.

Funding Information

The authors greatly acknowledge the support from the National Institutes of Health (R01 AR075143, R21 AR066320).

Supplementary Material

Supplementary Figure S1
Supplementary Figure S2

References

1. Censi, R., Di Martino, P., Vermonden, T., and Hennink, W.E. Hydrogels for protein delivery in tissue engineering. J Control Release **161,** 680, 2012.
2. Hoare, T.R., and Kohane, D.S. Hydrogels in drug delivery: progress and challenges. Polymer **49,** 1993, 2008.
3. Saul, J.M., and Williams, D.F. Hydrogels in regenerative medicine. In: Atala, A., Lanza, R., Thomson, J.A., Nerem, R.M. eds. Principles of Regenerative Medicine, Second Edition. London, UK: Elsevier, 2011, pp. 637–661.
4. Forero-Doria, O., Polo, E., Marican, A., *et al.* Supramolecular hydrogels based on cellulose for sustained release of therapeutic substances with antimicrobial and would healing properties. Carbohydrate Polym **242,** 116383, 2020.
5. Avila-Salas, F., marican, A., Pinochet., S., *et al.* Film dressings based on hydrogels: simultaneous and sustained-release of bioactive compounds with wound healing properties. Pharmaceutics **11,** 447, 2019.
6. Li, J., and Mooney, D.J. Designing hydrogels for controlled drug delivery. Nat Rev Mater **1,** 16071, 2016.
7. Vermonden, T., Censi, R., and Hennink, W.E. Hydrogels for protein delivery. Chem Rev **112,** 2853, 2012.
8. Nair, L.S. Injectable Hydrogels for Regenerative Engineering. London: Imperial College Press, 2016.

9. Moreira Teixeira, L.D., Feijen, J., van Blitterswijk, C.A., Dijkstra, P.J., and Karperien, M. Enzyme -catalyzed crosslinkable hydrogels: emerging strategies for tissue engineering. Biomaterials **33,** 1281, 2012.
10. Amini, A.A., Kan, H., Cui, Z., Maye, P., and Nair, L.S. Enzymatically cross-linked bovine lactoferrin as injectable hydrogel for cell delivery. Tissue Eng Part A **20,** 2830, 2014.
11. Narayanaswamy, R., and Torchilin, V.P. Hydrogels and there applications in targeted drug delivery. Molecules **24,** 603, 2019.
12. Mauri, E., Negri, A., Rebellato, E., Masi, M., Perale, G., and Rossi, F. Hydrogel nanoparticles composite system for controlled drug delivery. Gels **4,** 74, 2018.
13. Jain, E., Sheth, S., Dunn, A., Zustiak, S.P., and Sell, S. Sustained release of multicomponent platelet-rich plasma proteins from hydrolytically degradable PEG hydrogels. J Biomed Mater Res Part A **105,** 3304, 2017.
14. Huynh, V., and Wylie, R.G. Displacement affinity release of antibodies from injectable hydrogels. ACS Appl Mater Interfaces **11,** 30648, 2019.
15. Khanal, M., Gohil, S.V., Kuyinu, E., *et al.* Injectable nanocomposite analgesis delivery system for musculoskeletal pain management. Acta Biomater **74,** 280, 2018.
16. Buwalda, S.J., Vermonden, T., and Hennink, W.E. Hydrogels for therapeutic delivery: current developments and future directions. Biomacromolecules **18,** 316, 2017.
17. Skaalure, S.C., Akalp, U., Vernerey, F.J., and Bryant S.J. Tuning reaction and diffusion mediated degradation of enzyme-sensitive hydrogels. Adv Healthc Mater **5,** 432, 2016.
18. Lutolf, M.P., Lauer-Fields, J.L., Schmoekel, H.G., *et al.* Synthetic matrix metalloproteinase-sensitive hydrogels for the conduction of tissue regeneration: engineering cell-invasion characteristics. Proc Natl Acad Sci USA **100,** 5413, 2003.
19. Wade, R.J., Bassin, E.J., Rodell, C.B., and Burdick, J.A. Protease-degradable electrospun fibrous hydrogels. Nat Commun **6,** 6639, 2015.
20. Chandrawati, R. Enzyme responsive hydrogels for therapeutic delivery. Exp Biol Med **241,** 972, 2016.
21. Cheung, R., Ng, T.B., Wong, J.H., and Chan, W.Y. Chitosan: an update on potential biomedical and pharmaceutical applications. Mar Drugs **13,** 5156, 2015.
22. Paul, P., Kolesinska, B., and Sujka, W. Chitosan and its derivaties-Biomaterials with diverse biological activity for manifold applications. Mini Rev Med Chem **19,** 737, 2019.
23. Mu, M., Li, X., Tong, A., and Guo, G. Multi-functional chitosan based smart hydrogels mediated biomedical application. Expert Opion Drug Deliv **16,** 239, 2019.
24. Gohil, S.V., Brittain, S., Kan, H.M., Drissi, H., Rowe, D., and Nair, L.S. Evaluation of enzymatically crosslinked injectable glycol chitosan gel. J Mater Chem B **3,** 5511, 2015.
25. Hirai, A., Odani, H., and Nakajima, A. Determination of degree of deacetylation of chitosan by 1H NMR spectroscopy. Polym Bull **26,** 87, 1991.
26. Lavertu, M., Darras, V., and Buschmann, M.D. Kinetics and efficiency of chitosan reacetylation. Carbohydr Polym **87,** 1192, 2012.
27. Czechowska-Biskup, R., Jarosińska, D., Rokita, B., Ulański, P., and Rosiak, J.M. Determination of degree of deacetylation of chitosan-comparision of methods. Prog Chem Appl Chitin Deriv **17,** 5, 2012.
28. Taghizadeh, S.M., and Davari, G. Preparation, characterization, and swelling behavior of N-acetylated and deacetylated chitosans. Carbohydr Polym **64,** 9, 2006.
29. Dimzon, I.K.D., and Knepper, T.P. Degree of deacetylation of chitosan by infrared spectroscopy and partial least squares. Int J Biol Macromolcules **72,** 939, 2015.
30. Kubota, N., and Eguchi, Y. Facile preparaton of water soluble N-acetylated chitosan and molecular weight dependence of its water solubility. Polym J **29,** 123, 1997.
31. Montembault, A., Viton, C., and Domard, A. Rheometric study of the gelation of chitosan in aqueous solution with crosslinking agent. Biomacromolecules **6,** 653, 2005.
32. Hartl, L., Zach, S., and Seidl-Seiboth, V. Fungal chitinases: diversity, mechanistic properties and biotechnological potential. Appl Microbiol Biotechnol **93,** 533, 2012.
33. Paoletti, M.G., Norberto, L., Damini, R., and Musumeci, S. Human gastric juice contains chitinase that can degrade chitin. Ann Nutr Metab **51,** 244, 2007.
34. Kzhyshkowska, J., Gratchev, A., and Goerdt, S. Human chitinases and chitinase-like proteins as indicators for inflammation and cancer. Biomarker Insights **2,** 128, 2007.
35. Qasim, S.B, Husain, S., Huang, Y., *et al.* In vitro and *in vivo* degradation studies of freeze gelated porous chitosan composite scaffolds for tissue engineering applications. Polym Deg Stab **136,** 31, 2017.
36. Azab, A.K., Doviner, V., Orkin, B., *et al.* Biocompatibility evaluation of crosslinked chitosan hydrogels after subcutaneous and intraperitoneal implantation in the rat. J Biomed Mater Res A **83,** 414, 2007.
37. Costa-Pinto, A.R., Martins, A.M., Castelhano-Carlos, M.J., *et al.* In vitro degradation and *in vivo* biocompatibility of chitosan–poly(butylene succinate) fiber mesh scaffolds. J Bioactive Compatible Polym **29,** 137, 2014.
38. Tomihata, K., and Ikada, Y. *In vitro* and in vivo degradation of films of chitin and its deacetylated derivatives. Biomaterials **18,** 567, 1997.
39. Ganesh, N., Hanna, C., Nair, S.V., and Nair, L.S. Enzymatically cross-linked alginic-hyaluronic acid composite hydrogels as cell delivery vehicles. Int J Bio Mac **55,** 289, 2013.

Address correspondence to:
Lakshmi S. Nair, MPhil, PhD
Department of Orthopaedic Surgery
University of Connecticut Health Center
415 Lane Road, Rm 2129, MR5
Farmington, CT 22908
USA

E-mail: nair@uchc.edu

Received: July 20, 2020
Accepted: August 27, 2020
Online Publication Date: October 15, 2020